Comparative study for physical properties and corrosion mechanism of synthetic and *in situ* $MgAl_2O_4$ spinel formation zero cement refractory castables

Y. K. Kalpaklı*

Magnesium aluminate spinel ($MgAl_2O_4$) is an excellent castable refractory product due to its high temperature thermal, chemical and mechanical properties. Alumina spinel castables are produced by addition of synthetic spinel or *in situ* spinel formation during the firing process. In the first part of the experimental studies, alumina rich $MgAl_2O_4$ spinel castable was produced using a solid state reaction technique. Tabular alumina and sea water magnesia (<100 μm) were used as starting raw materials. In the second part of the experimental studies, commercial synthetic spinel added castables were produced. In order to compare experimental results, both parts of the experimental study involved compositions with the same proportions of MgO. α-500 hydratable alumina was used as binder. Castables were sintered at 1500 and 1600°C. Water absorption, apparent porosity, bulk density and cold crushing strength values were considered and the optimum sintering temperature, proportions of synthetic spinel and sea water magnesia were determined. The XRD patterns confirm the phase formation of $MgAl_2O_4$. Moreover, the physical properties of the castables were supported by this XRD analysis. Scanning electron microscopy investigations of the fired samples were carried out to compare the effect of synthetic spinel addition and *in situ* phase formation on the physical properties of the castables. The mechanism of slag penetration to two types of zero cement castables for steel ladles was examined and the penetration layer chemically analysed by energy dispersive X-ray analysis studies.

Keywords: Sintering, Electron microscopy, Slag corrosion, Hydratable alumina, *In situ* spinel formation

Introduction

Spinel containing refractories such as MgO-$MgAl_2O_4$ and Al_2O_3-$MgAl_2O_4$ are widely used refractories.[1–6] Spinel bonded Al_2O_3-$MgAl_2O_4$ castables, which possess superior properties in terms of slag penetration and structural spalling, have been successfully used as major lining materials in steel ladles.[7]

A number of techniques such as conventional oxide mixing or solid–solid reaction have been employed for preparation of spinel $MgAl_2O_4$.[1] Magnesium aluminate spinel is industrially produced from magnesia and alumina or from magnesite and bauxite[8] by fusion or sintering at high temperatures up to 1750°C. It is difficult to produce ultra fine and reactive spinel powders. For this reason, various non-convensional methods, such as coprecipitation,[9–11] sol–gel,[12–16] spray drying,[17] spray pyrolysis,[18,19] freeze drying,[20] flame spraying pyrolysis[20] and mechanochemical techniques,[20] have been used for preparing reactive spinel powders. In general, the spinel powders prepared by these methods show high purity and small particle size, when compared with spinel powders produced by the conventional solid state reaction methods.[20]

Commercial sintered magnesia spinel refractory materials are divided in to three categories: magnesia rich, stoichiometric and alumina rich. Castables with addition of alumina rich spinel with 90%Al_2O_3 content are better in terms of slag penetration than those with stoichiometric or magnesia rich spinel additions.[21,22]

Spinel is developed in refractories by four ways:

(i) as preformed synthetic spinel powder in the matrix
(ii) as preformed spinel aggregates
(iii) as *in situ* spinel formed by adding Al_2O_3 to MgO based refractories or MgO to Al_2O_3 based refractories
(iv) as *in situ* spinel formed by addition of a mixture of MgO and Al_2O_3 powders.[1]

Department of Chemical Engineering, Faculty of Chemistry and Metallurgy, Yıldız Technical University, Istanbul, Turkey

*Corresponding author, email yaseminkalpakli@gmail.com

© 2009 Institute of Materials, Minerals and Mining
Published by Maney on behalf of the Institute
Received 23 May 2009; accepted 6 July 2009
DOI 10.1179/030192309X12506804200546

Synthetic spinel is an expensive material, therefore refractory production by *in situ* spinel formation with free MgO addition is relatively economical.

The using of hydratable alumina, which has less than 0·1 wt-%CaO, instead of cement is a new trend in castable refractory production. The advantages of zero cement castables (ZCC) over low cement or ultra low cement castables are enhanced hot properties and slag resistance.[23]

A new generation hydraulic binder, hydratable alumina, is based on the amorphous mesophase of transition of alumina (ρ-alumina) which reacts with water to form a hydraulic bond. Hydratable alumina can be produced either by dehydration of Gibbsite in vacuum at 600°C or by a brief contact with hot air blast at 600 to 900°C. A commercial available hydratable alumina contains ~60% ρ-alumina, a small content of χ-alumina and residual aluminum hydroxide (Gibbsite).

ρ-alumina reacts with water at room temperature by the following process[24]

$$2\rho\text{-}Al_2O_3 + (4+x)H_2O \rightarrow$$

$$Al_2O_3.3H_2O + Al_2O_3(1+x)H_2O \quad (x=0\ldots1)$$

Bayerite Bohemite gel

Interlocking bayerite crystals and gel confer green mechanical strength on the refractory structure by filling pores and interfacial defects and by forming honeycomb structures on the surface of aggregates, attaching adjacent grains to each other and to the surrounding matrix.[24,25]

Zero cement castables containing hydratable alumina binders are now being used extensively in the electric furnace delta section, metal treatment lances, continuous caster dams, weir and impact pads and ladle impact pads and well blocks.[26] They may also be used in field cast monolithic lining where firing is carefully controlled.[27]

The lifetime of the castables is limited by their wear rate arising from slag penetration,[28] so that explaining the mechanism of slag penetration is important for their users.

In alumina spinel refractories, the stoichiometry of the spinel used strongly influences the penetration area of slag on the castable. Castables with alumina rich spinel increase the resistance to slag penetration and wear.[22,29]

Ko[30] indicated that penetration is decreased with increased MgO content in spinel and believed that the dissolution of spinels and precipitation of MgO in the penetrating slag result in an effective increase in the viscosity of the penetrating slag and hence the penetration is lessened.

The crystal structure of magnesium aluminate spinel can accommodate high levels of deleterious elements such as Fe and Mn from slags without loss of structural integrity.[31]

Mori *et al.*[7] explained that for a slag composed mainly CaO–FeO–SiO_2, CaO in the slag reacts primarily with Al_2O_3 to form CaO–Al_2O_3 compounds while the FeO forms solid solution in the spinel. Slag composition moves to a SiO_2 rich composition and the penetration layer rises. However, liquid phase viscosity also rises and hence further penetration is blocked.

Nagai *et al.*[31] stated that penetration is blocked because of rises in both the melting point and viscosity of the slag based on the phase diagram of CaO–FeO–SiO_2.

Fujii *et al.*[22] observed that using alumina rich spinel the peeling damage to the steel ladle lining is lessened.

In this study synthetic and *in situ* spinel formation in ZCCs containing MgO in similar proportion were sintered at 1500 and 1600°C. The optimum sintering temperature and the best proportion of synthetic spinel and sea water magnesia were determined by investigating the physical properties such as water absorption, apparent porosity, bulk density and cold crushing strength (CCS) in the ZCCs. The effects of slag penetration on the two types of ZCC product were investigated.

Experimental

Properties of raw materials

In this work, alumina with various particle size produced by Almatis Industrial Chemicals (Germany) was mixed with sea water magnesia (origin China) to form the blend. α-500 hydratable alumina was used as a binder.

X-ray fluorescence analysis of sea water magnesia was conducted in a Spectro-IQ2 system using Breıtlander Autofluxer fusion equipment. These analysis results are given Table 1 as chemical composition of sea water magnesia and hydratalte alumina.

The particle size distributions of tabular alumina, reactive alumina, calcined alumina and α-500 hydratable alumina were measured in a Malvern Mastersizer 2000 (Malvern, Germany) instrument. These analysis results are given in Fig. 1.

The characteristic features of alumina rich synthetic spinels (AR-78) and hydratable alumina by Almatis Industrial Chemicals are given in Table 2.

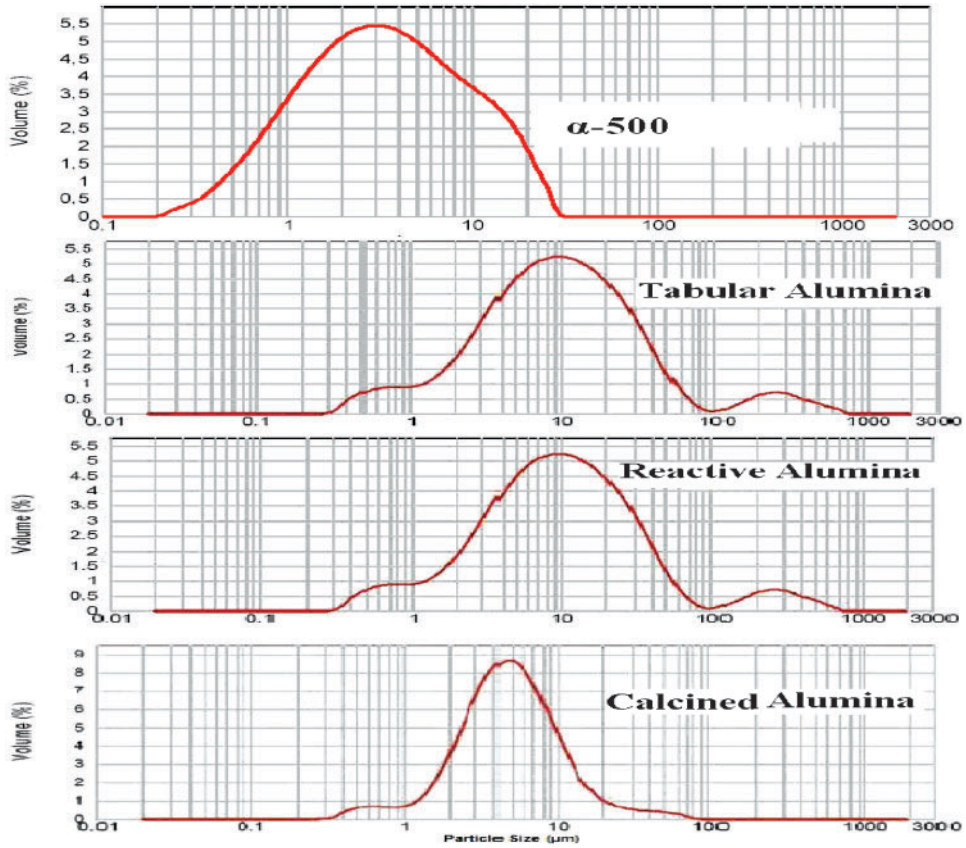
Preparation of samples

The Andreassen equation was used to determine the ratio of the range of the particle size of raw material and particle size distribution parameter q. This was found to be 0·26 for vibratory castables in a previous study.[32]

Various proportions of sea water magnesia (3, 4, 5, 6 and 7 wt-%MgO given identification M3, M4, M5, M6 and M7) were added to the mixtures listed in Table 3 for *in situ* $MgAl_2O_4$ spinel formation. Moreover, various proportions of alumina rich spinel AR-78 (15, 20, 25, 30

Table 1 Chemical composition of sea water magnesia and hydratable alumina

Raw material	Composition, wt-%	
Sea water magnesia	MgO	98·8
	Al_2O_3	0·054
	SiO_2	0·09
	CaO	0·065
	Fe_2O_3	0·22
	Cr_2O_3	0·08
	Na_2O	<0·11
α-500 hydratable alumina	Al_2O_3	83·0
	CaO	0·60
	Na_2O	0·30
	SiO_2	0·30
	Physical properties	
	Lost of humidity (25–250°C), %	6·50
	Lost of mass (250–1100°C), %	9·20



1 Particle size distribution of tabular alumina, reactive alumina, calcined alumina and α-500 hydratable alumina

and 35 wt-% spinel given identification A15, A20, A25, A30 and A35) were added to the mixtures listed Table 4.

The magnesia grain size is an important parameter to the production of *in situ* spinel castable.

Coarse magnesia grains do not react with alumina and cracks can develop due to the thermal expansion mismatch between magnesia and spinel.[33] Therefore, the magnesia grain size was selected as (<100 μm) in this study.

The particle size distribution and mass contents of these mixtures are listed in Table 3 and 4. Each mixture is firstly dry mixed in a Hobart A200 mixer for 2 min. Afterwards water is added and wet mixing is carried out for ~5 min. The homogenised mixture is cast into moulds of $5 \times 5 \times 5$ cm on a vibrating table with 50 Hz vibrating rate. The samples are kept for 24 h at room temperature for one day and then cured at a temperature of 110°C for 24 h in a Binder type incubator. The refractory samples were sintered in two different groups at a temperature of either 1500 or 1600°C for 5 h in a NaberTherm (Germany), direct heater furnace at heating speed of 5°C min^{-1}. After firing, porosity, bulk density, CCS and slag tests were carried out. Apparent porosity and bulk density were measured by the water immersion method according to DIN 51056 standard. The CCS tests were done according to DIN 51067 standard. Cold crushing strength tests were carried out in a 200 tone hydraulic press (Atom Technique, Turkey).

Table 2 Characteristic of synthetic alumina rich spinel additives

Raw material	Composition, wt-%	
Alumina rich spinel (AR-78)	Al_2O_3	76·87
	MgO	22·5
	CaO	0·24
	SiO_2	0·10
	Na_2O	0·09
	Fe_2O_3	0·15
	Fe magnetic	0·05
	Physical properties	
	Bulk specific gravity, g cm^{-3}	3·3
	Apparent porosity, %	1·8
	Water absorption, %	0·5

X-ray diffraction (XRD) experiments were conducted with Philips PANalytical X'Pert PRO X equipment using the setting of 45 mA and 40 kV at a 2θ range 0–90°.

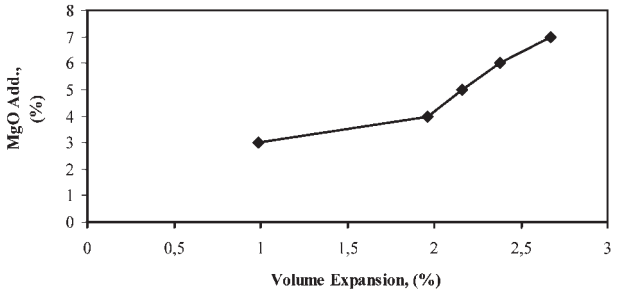
Scanning electron microscopy (SEM) investigations were carried out in JEOL T-330 SEM operated at 20 kV and linked with a Noran energy dispersive spectrometer (EDS) attachment.

Results and discussion

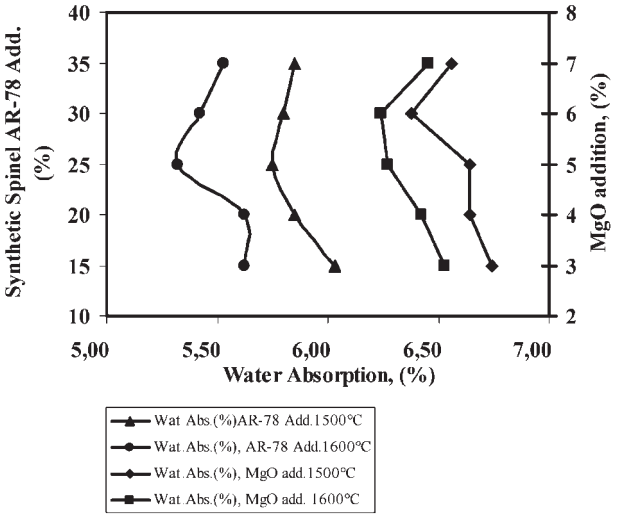
Physical and mechanical properties

Effect of MgO and synthetic spinel (AR-78) addition on water adsorption, porosity and bulk density

The alumina magnesia spinel compositions based on tabular alumina have no free silica in their compositions and for this reason do not allow the formation of phases with low melting point such as cordierite. They have the characteristic of thermal expansion with high stability.



2 Variation in volume expansion with MgO addition, %

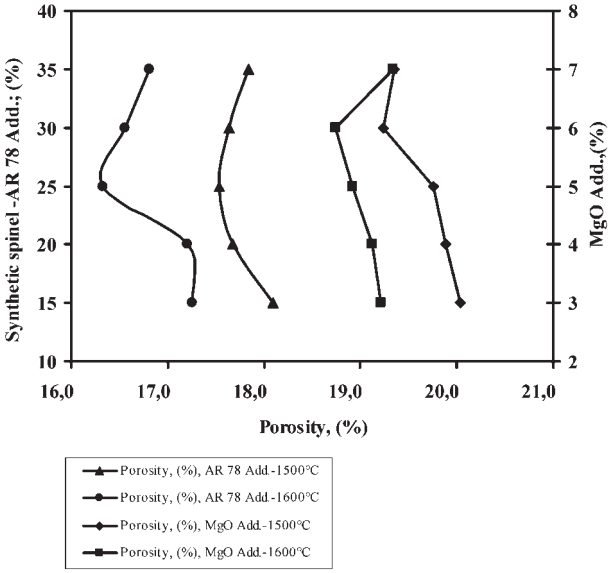


3 Water absorption values as function of additive type and percentage

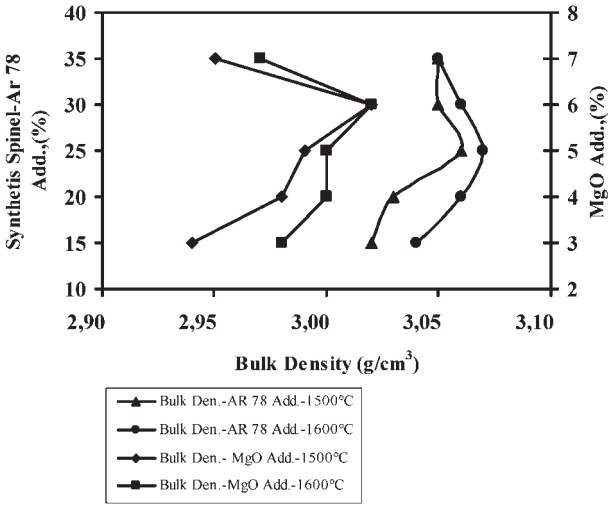
At this stage of the study, raw materials including high purity alumina and magnesia are examined and their volumetric expansion rates are studied. In the materials rich in alumina and with spinel formation the amount of MgO addition that yields the best refractory properties has been determined. Variation in volume shrinkage (%) for all proportions of synthetic spinel (AR-78) additions was 0·5%.

Variation in volume expansion (%) with MgO addition is given in Fig. 2.

Physical properties of refractories are important parameter for determined and selection of application area and indicate the lifetime of the castables and their wear rate from slag penetration.[34]



4 Porosity values as function of additive type and percentage



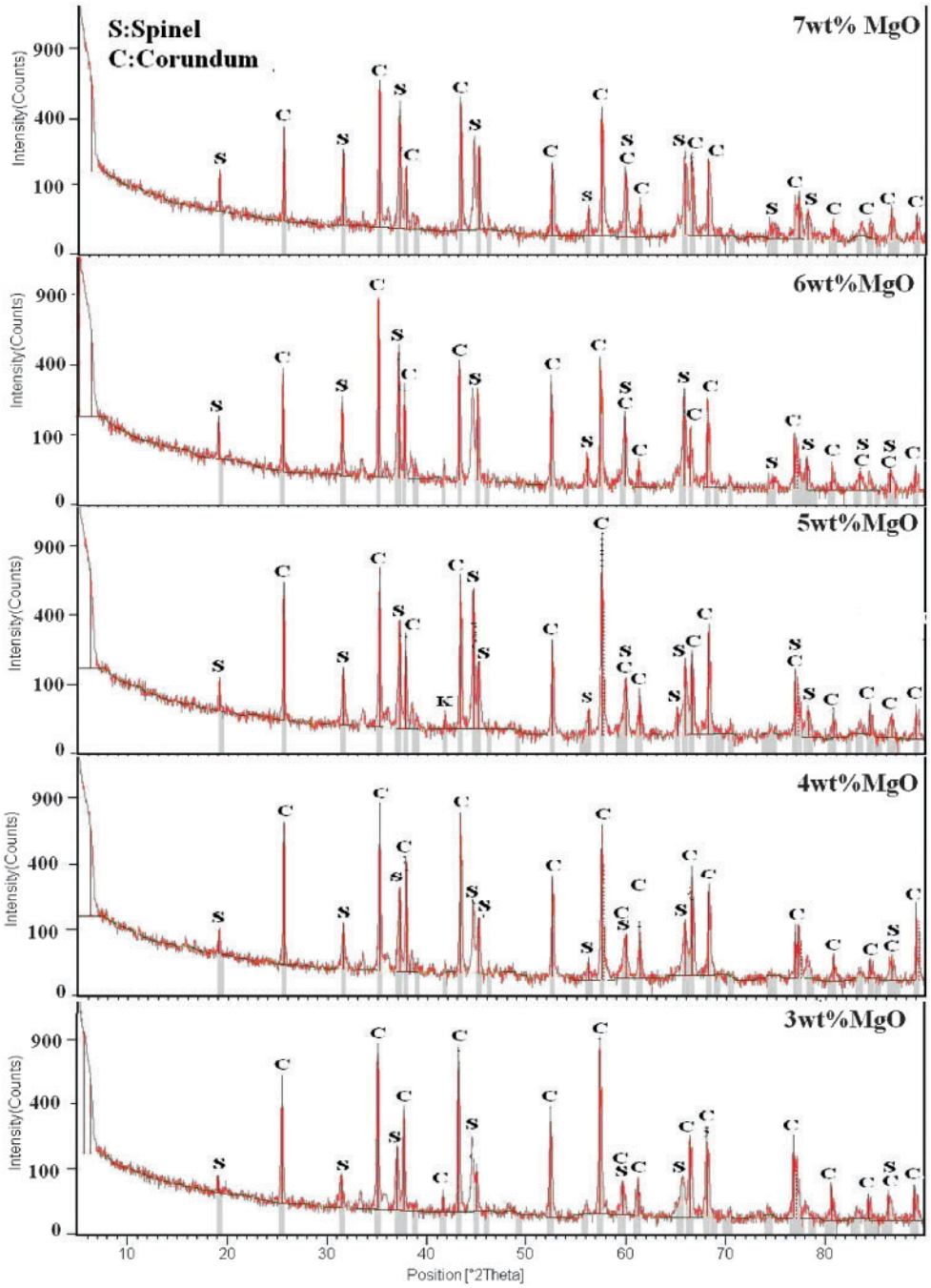
5 Bulk density values as function of additive type and percentage

The effects of MgO and synthetic spinel (AR-78) additions on the water adsorption, porosity and bulk density values for the samples sintered at 1500–1600°C are indicated in Figs. 3–5.

It is seen that the values of water absorption, porosity and bulk density of synthetic and *in situ* $MgAl_2O_4$ spinel samples change similarly with each other. The increasing

Table 3 Particle size distribution and mass contents of sea water magnesia added (M3-7) and free from sea water magnesia (M0) castables

Raw materials	Particle size, mm	M0, wt-%	M3, wt-%	M4, wt-%	M5, wt-%	M6, wt-%	M7, wt-%
Tabular alumina	1–6	37·20	37·20	37·20	37·20	37·20	37·20
Tabular alumina	0·04–1	35·60	34·60	34·27	33·93	33·60	33·27
MgO	0·04–0·1	…	1·00	1·33	1·67	2·00	2·33
MgO	−0·04	…	2·00	2·67	3·33	4·00	4·67
Tabular alumina	−0·04	12·20	10·20	9·53	8·87	8·20	7·53
Reactive alumina	−0·04	7·00	7·00	7·00	7·00	7·00	7·00
Calcined alumina	−0·04	4·97	4·97	4·97	4·97	4·97	4·97
α-500	−0·04	3·00	3·00	3·00	3·00	3·00	3·00
Dispersant	…	0·03	0·03	0·03	0·03	0·03	0·03

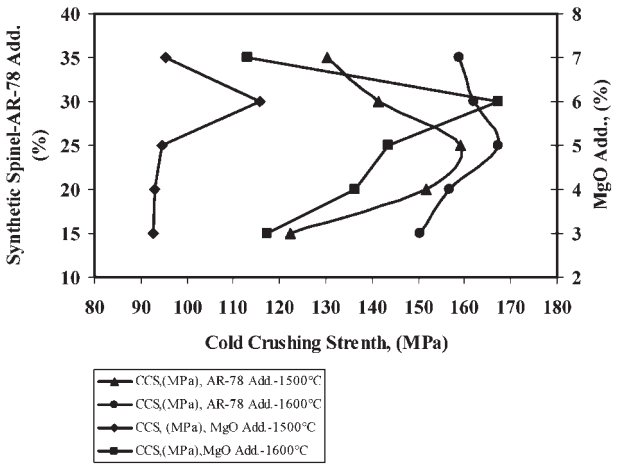


6 X-ray diffraction pattern of MgO added castables sintered at 1600°C

of the sintering temperatures from 1500 to 1600°C has influenced these specifications positively. The samples with synthetic spinel additions when compared to the spinel samples with *in situ* formation are seen to have lower rates of porosity and water absorption but higher rates of bulk density.

Table 4 Particle size distribution and mass contents of alumina rich synthetic spinel added (A15–35) and free from synthetic spinel (A0) castables

Raw materials	Particle size, mm	A0, wt-%	A15, wt-%	A20, wt-%	A25, wt-%	A30, wt-%	A35, wt-%
Tabular alumina	1–6	37·20	37·20	37·20	37·20	37·20	37·20
Tabular alumina	0·04–1	35·60	32·80	27·80	22·80	9·37	9·37
Tabular alumina	−0·04	12·20	…	…	…	8·43	3·43
alumina rich synthetic spinel (AR-78)	−0·04	…	15·00	20·00	25·00	30·00	35·00
Reactive alumina	−0·04	7·00	7·00	7·00	7·00	7·00	7·00
Calcined alumina	−0·04	4·97	4·97	4·97	4·97	4·97	4·97
α-500	−0·04	3·00	3·00	3·00	3·00	3·00	3·00
Dispersant	…	0·03	0·03	0·03	0·03	0·03	0·03



7 Cold crushing strength values as function of additive type and percentage

The percentage of synthetic spinel chosen by considering the MgO amounts which are added into the mixture to get *in situ* $MgAl_2O_4$ spinel formations, the best values of water absorption, porosity and bulk density are obtained with the addition of 25% (A25) synthetic spinel.

In the *in situ* spinel samples as the MgO addition increases porosity and water absorption values parallel to the increase in $MgAl_2O_4$ spinel amount it has been suggested that it decreases a bit and gives the optimum value of 6% with MgO (M6) addition. Bulk density has, on the other hand, reached the value of $\sim 3{\cdot}05$ g cm^{-3} of 25% (A25) synthetic spinel samples including the same amount of MgO as the value $3{\cdot}02$ g cm^{-3} in the samples that are sintered at 1600°C with the addition of 6%MgO.

The increase during the *in situ* spinel formation in samples has been determined as a result of XRD examination with the MgO increase from 3 to 7% in castable refractory from which $MgAl_2O_4$ spinel formulation is provided (Fig. 6). However, the increase during the *in situ* spinel formation in samples leads to the volume expansion as well as an increase in the porosity.[35,36] On the other hand, the formation of brucite in the form of castable refractory by reacting with the magnesia at the heats 150–200°C while it is vaporising and removing from the structure during the water drying process included in the castable refractory structure.[37,38] As a result of this reaction 5% of volume expansion occurs in the castable refractory.[38,39] This causes porosity increase in the reactions and it hinders the material to obtain a more dense structure during sintering.[39]

Effect of MgO and synthetic spinel (AR-78) addition on mechanical properties

In samples consisting of *in situ* $MgAl_2O_4$ spinel, porosity and water adsorption values are obtained that are a bit higher in comparison with the samples with synthetic spinel additions because of volume expansion occurred from formation of spinel and hydration of magnesia. However, when the values of CCS is examined, with increasing the percentage of MgO addition, it is clearly understood from Fig. 7 that the CCS values of the samples increase too. Moreover, it is seen that these values reach the maximum rate with the addition of 6%MgO.

As a result of the physical and mechanical tests it has been concluded that the porosity rise increases parallel the rise in MgO and that it reaches the highest values in castable samples with 7%MgO additions. When the CCS test results are examined, it has been determined that *in situ* spinel phase has the positive effect until 6%MgO but in the 7%MgO content CCS decreases as a result of the negative effects of the both brucite formed due to the moisture around and porosity rise.

Increased strength together with increased porosity of $MgAl_2O_4$ is believed to be an indication that this material has a higher yield strength and lower rigidity in comparison with α-Al_2O_3.[40] Therefore, the hardness of spinel alumina composite decreases while ductility and strength increases.

Phase analysis

Figure 6 shows XRD pattern of the MgO added castable samples after sintering at 1600°C. From this figure, it is seen that *in situ* spinel phase formation increases with increasing MgO. There is no periclase phase determined as all of the magnesia reacts with alumina and spinel phase were formed. Gradual increase in spinel phase peak intensity and decrease in corundum phase have been observed with increasing spinel content.

X-ray diffraction analyses of castables supported physical properties results taken from MgO added samples are given Figs. 3–5 and 7. *In situ* spinel phase formation is responsible for improving the CCS values and corrosion resistance of castable.[41]

Slag corrosion resistance (crucible method)

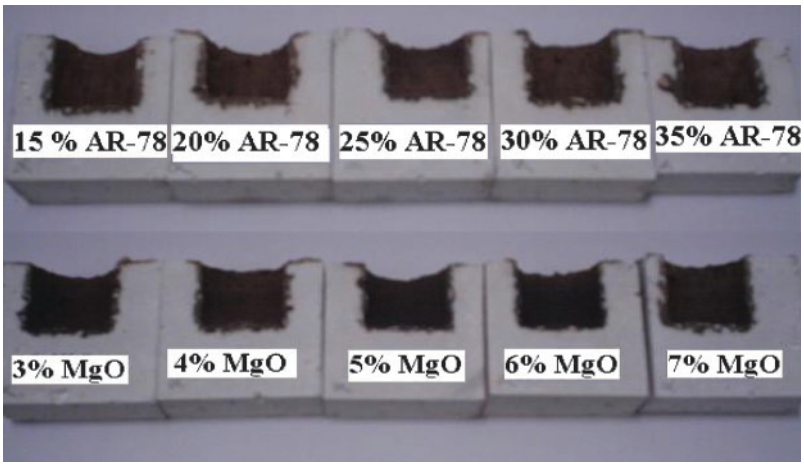
Ladle slag of steel plant supplied from the steel plant of Erdemir Inc. has been utilised in the corrosion tests of the castable samples. The chemical composition of this slag is given in Table 5 ($CaO/SiO_2=2.29$). The slag which is composed mainly of $CaO–Al_2O_3–SiO_2$ contains 17·66% iron solution ($FeO+Fe_2O_3$). It has been granulated and sifted in the 100 μm sieve. The powdered slag under the sieve has been separated in order to be used in the corrosion test.

The slag charge was applied to the inside of the castable crucible pot samples prepared according to DIN 51069 and sintered at 1600°C for 4 h in a Naber Therm (Germany) type furnace at a heating rate of 10°C min^{-1}. Castable samples which had interacted with the slag were cut as stated in DIN 51069 and their corrosion surfaces were examined.

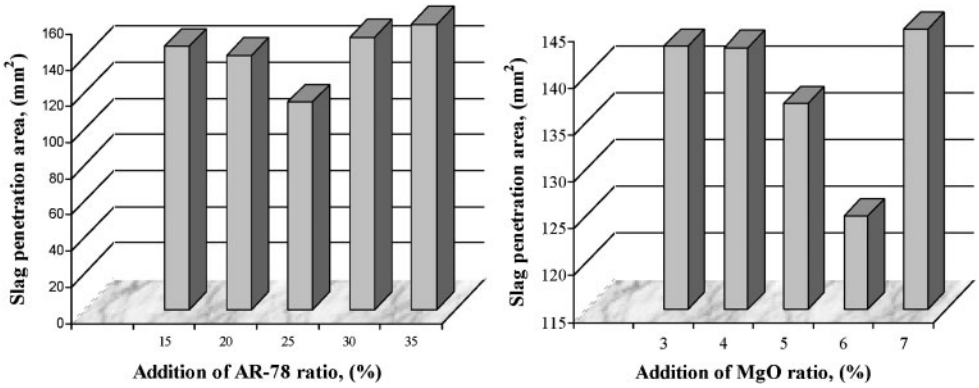
An intense slag region comprising dissolution and infiltration areas was observed at the interfaces (Figs. 8 and 9). For comparison of the slag infiltration in samples A25 and M6, slag infiltration areas were measured using semiquantitative graph measurement

Table 5 Chemical composition of ladle slag (C/S=2·29)

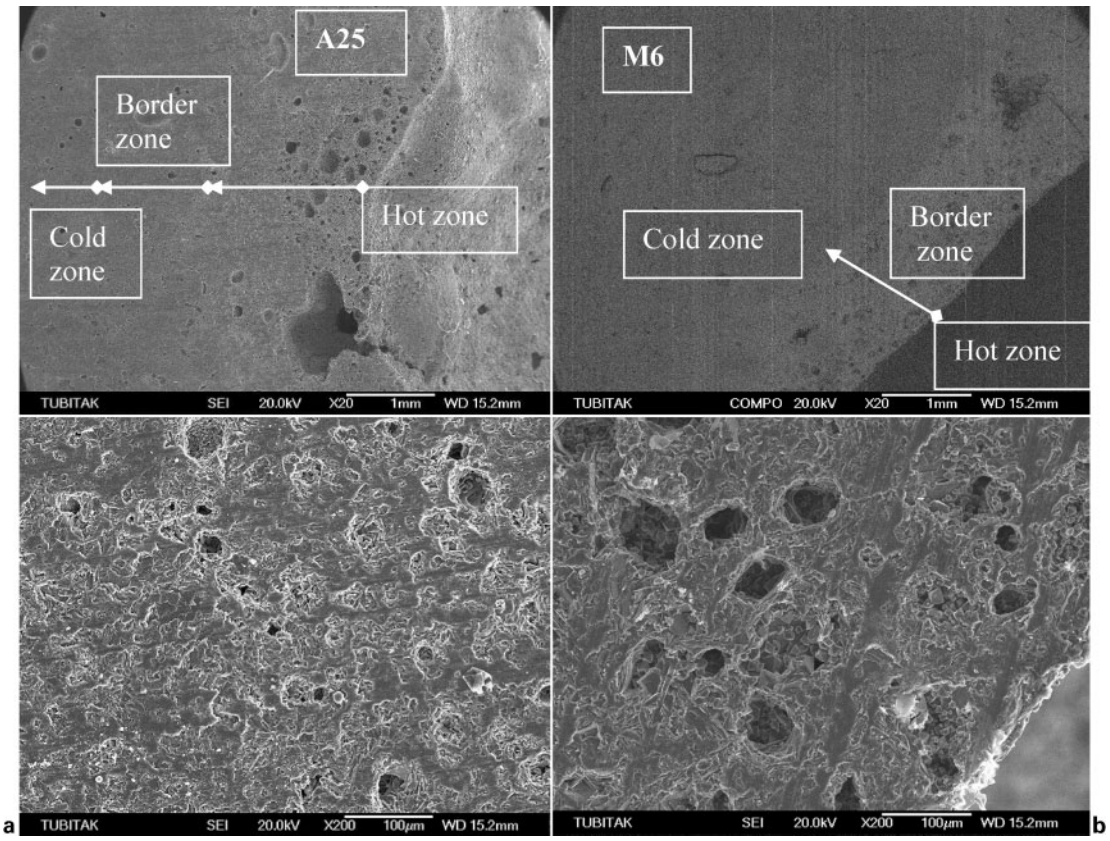
	FeO/Fe_2O_3	SiO_2	MnO	Al_2O_3	CaO	MgO	P_2O_5	S	Na_2O	K_2O	TiO_2	Cr_2O_3
wt-%	17·66	14·32	4·62	14·02	32·87	7·01	0·617	0·221	0·001	0·107	0·483	0·114



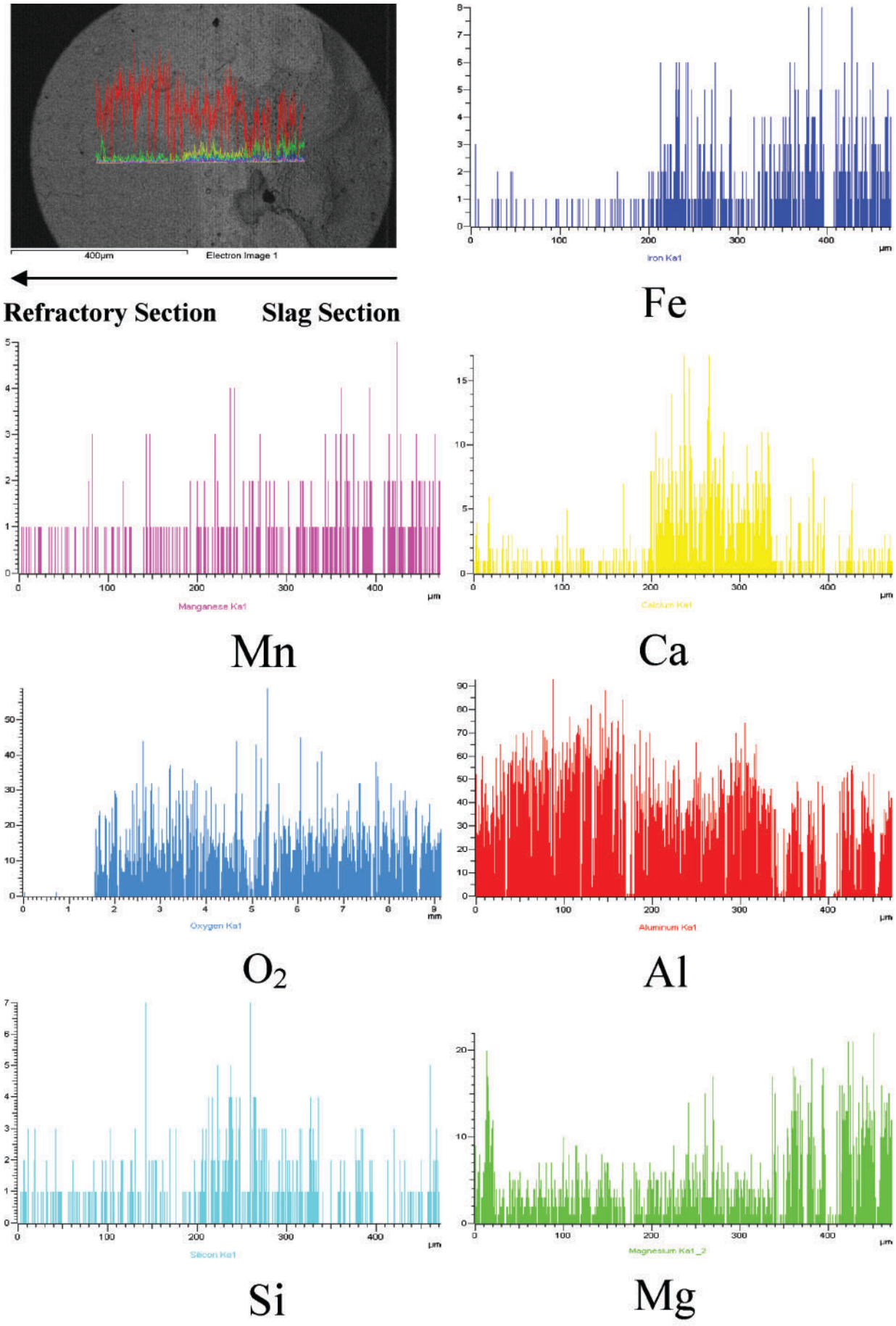
8 Slag penetration areas images of castables containing AR-78 and MgO additive at 1600°C



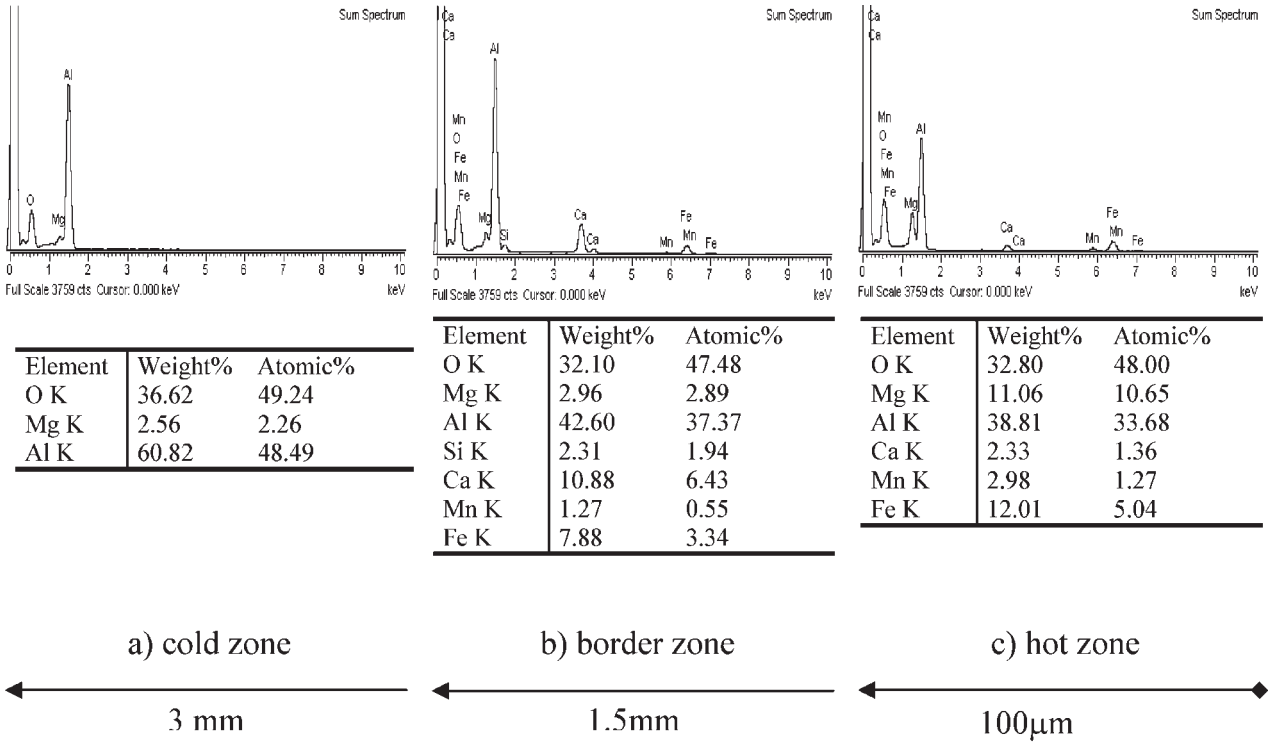
9 Slag penetration areas of castables containing AR-78 and MgO additive at 1600°C



10 Image (SEM) of sample *a* A25 and *b* M6 ×20



11 Elemental distribution analysis of slag penetration layer along line in A25 castable



Element	Weight%	Atomic%
O K	36.62	49.24
Mg K	2.56	2.26
Al K	60.82	48.49

Element	Weight%	Atomic%
O K	32.10	47.48
Mg K	2.96	2.89
Al K	42.60	37.37
Si K	2.31	1.94
Ca K	10.88	6.43
Mn K	1.27	0.55
Fe K	7.88	3.34

Element	Weight%	Atomic%
O K	32.80	48.00
Mg K	11.06	10.65
Al K	38.81	33.68
Ca K	2.33	1.36
Mn K	2.98	1.27
Fe K	12.01	5.04

12 Energy dispersive spectroscopy point analysis of slag penetration layer of sample A25 (marked in Fig. 10*a*)

paper. As shown in Fig. 9, slag infiltration of castable containing AR-78 (A25) additive was slightly lower than MgO additive castable (M6). However, it can be noted that the slag infiltration of castable M6, although it had higher porosity, was equal to that of castable A25 at 1600°C.

To examine the slag corrosion in detail, castables A25 and M6 corroded at 1600°C were investigated.

Figure 10*a* shows a SEM image of the slag region. Figure 11 shows elemental distribution analysis of slag penetration layer along the line in A25 castable and Fig. 12 shows the EDS point analysis extending from the slag contact zone of the same region to the inner sections of the refractory and gives the corresponding chemical composition of sample A25. Results of EDS in the figure are taken from the corroded zone (hot zone), uncorroded refractory zone (cold zone) and border between the hot and cold zones (border zone).

Figures 10*b*, 13 and 14 show sectional image and details of castable crucible M6.

The effect of the slag on the materials can be explained as the components with low melting points increase the activity of the slag so that it eases the penetration to the materials.

Findings using SEM-EDS are given in Figs. 10 and 12.

Figure 14 shows the complex compound of $(Fe,Mn)(Fe,Al)_2O_4$ is formed as a result of the chemical reactions between Fe^{3+}, Fe^{2+} and Mn^{2+} ions existing in the hot zone of ZCC.

Castables with high alumina, including synthetic (AR-78) and *in situ* $MgAl_2O_4$ spinel's

$$MgO{\cdot}Al_2O_3 + (n-1)Al_2O_3 \rightarrow MgO{\cdot}nAl_2O_3 \quad (1)$$

It has a lattice structure which has cation vacancies as is due to reaction (1). These vacancies allow easy infiltration of Fe and Mn ions, so that the stability of the structure is protected and it resists very well against the slag attacks,[42] i.e. the concentration of Fe and Mn decreases and their expansion to deeper areas is hindered.

When the results of EDS analysis is examined, the influence of Fe, Mn, Ca and Si ions likely to diffused from the slag in hot zone is clearly seen. This diffusion continues until the border zone.

As a result of the slag analysis, it has been proposed that castable refractories with 6%MgO (M6) addition show a very high slag corrosion resistance at 1600°C. As a result of the SEM-EDS analysis given in Fig. 14*b* it is seen that a ~1 mm slag diffuses from hot zone to cold zone. On the other hand when we look at the results of SEM-EDS analysis of the samples with 25% synthetic spinel addition (A25) in Fig. 12*b*, we can see that a ~1·5 mm slag diffuses from hot zone to cold zone.

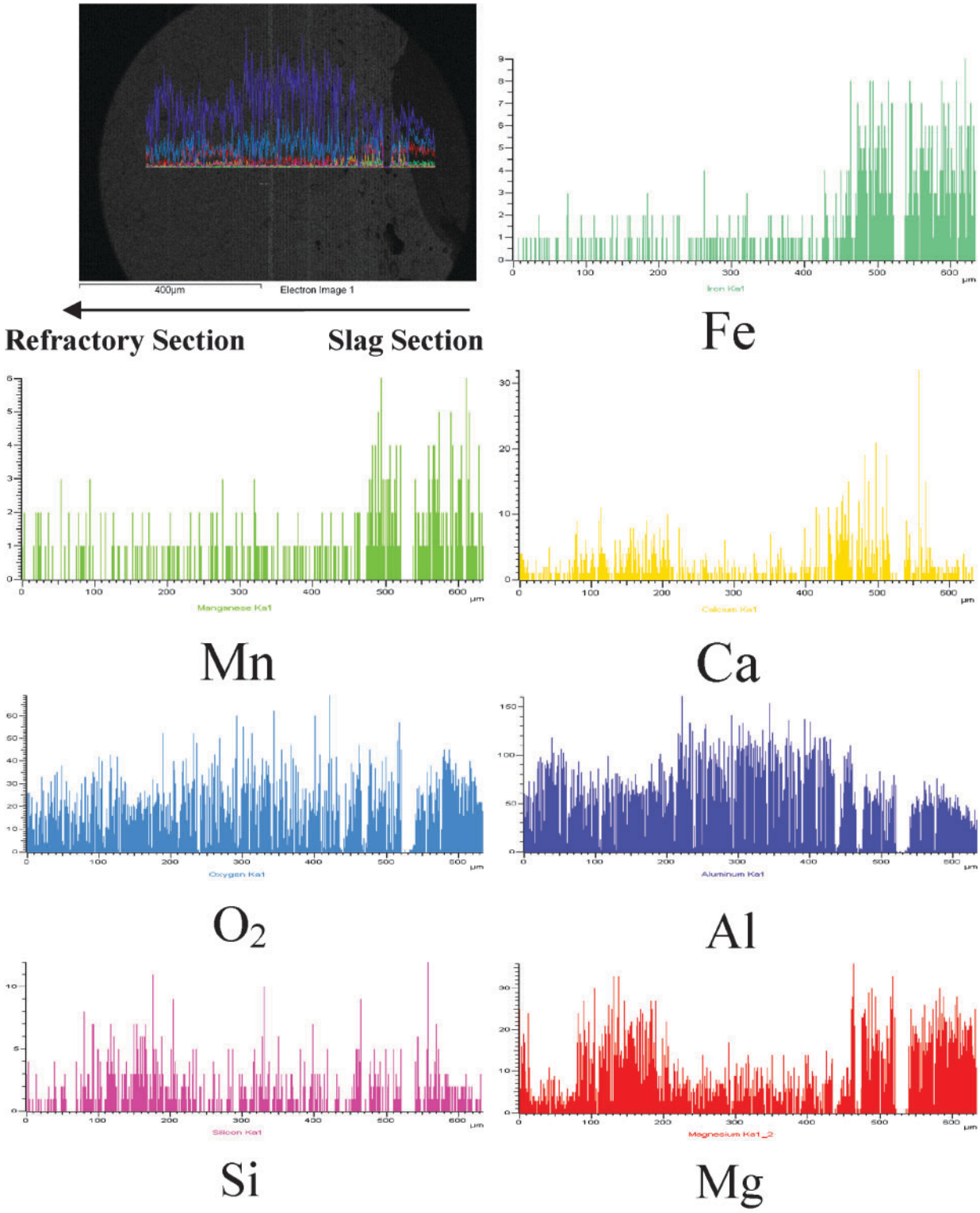
It can be clearly seen in Figs. 12–14 in the EDS results that Fe and Mn diffusion in castables with synthetic spinel addition in hot zone are higher than that in the *in situ* spinel samples.

In the EDS analysis, the M6 sample in hot zone cannot resist against Fe and Mn attacks and it allows formation of Fe and Mn spinel due to the damage of its lattice structure. With this formation, the diffusion of Fe and Mn ions slows down and the activation ends at a point that can be regarded as an early time. As is seen in Fig. 14, no Fe and Mn is found in ~2 mm depth from the hot zone; but MgO entity is determined in that zone.

In the EDS analysis of A25 samples with synthetic spinel addition, as can be seen in Fig. 12*a*, no Fe and Mn has occurred in ~3 mm depth from the hot zone.

Conclusions

Alumina magnesia synthetic spinel which is commonly used in impact pads of steel melting ladles and ladle



13 Elemental distribution analysis of slag penetration layer along line in M6 castable

refractory linings is an expensive material, thus alumina magnesia spinels formed *in situ* tend to be used instead of the castables containing synthetic spinel. Thereby environmental pollution can be avoid by reducing energy consumption

In this study characteristics and slag resistances of synthetic and *in situ* spinel formation ZCC containing MgO in same portions were analysed comparatively.

1. X-ray diffraction analyses confirmed that MgO and Al_2O_3 have reacted together and converted to $MgAl_2O_4$ spinel after sintering at 1600°C in *in situ* spinel formation castables.

2. Physical and mechanical properties of the MgO–Al_2O_3 castables are significantly affected by MgO and synthetic spinel addition ratio in the mixture.

3. *In situ* spinel castable with 6 wt-%MgO addition shows much better resistance to iron basic slag attack than high cost 25 wt-% synthetic spinel added castables.

4. Alumina based, cement free, *in situ* spinel castables have been developed and optimised to be conferred with stronger resistance to basic ferritic slag attack.

Acknowledgements

I would like to thank Superateş Refractories Company for their support throughout this investigation. This study was supported by YTÜ BAPK project no. 24-07-01-04 as industrial project.

References

1. S. Zhang and W. E. Lee: 'Refractories handbook', 215–257; 2004, New York, Marcel Dekker Inc.
2. J. McColm: 'Ceramic science for materials technologist', 229–306, 1983, London, Blackie & Son Ltd.
3. A. Koller: 'Structure and properties of ceramics', 309–311, 1994, New York, Elsevier.
4. M. A. Alper: 'High temperature oxides', 77–146, 1971, New York, Academic Press.
5. S. Banerjee: 'Monolithic refractories: a comprehensive handbook', 33–34; 1998, Singapore, World Scientific Publishing.
6. in 'Refractories handbook', 163–164; 1998, Tokyo, The technical Association of Refractories.
7. J. Mori, N. Watanabe, M. Yoshimura, Y. Oguchi and T. Kawakami: *Ceram. Bull.*, 1990, **69**, (7), 1172–1176.
8. F. N. Cunha-Duncan and R. C. Bradt: *J. Am. Ceram. Soc.*, 2002, **85**, (12), 2995–3003.
9. J. Guo, H. Lou, H. Zhao, X. Wang and Z. Xiaoming: *Mater. Lett.*, 2004, **58**, 1920–1923.
10. G. Gusmano, P. Nunziante, E. Traversa and G. Chiozzini: *J. Eur. Ceram. Soc.*, 1991, **7**, (1), 31–39.
11. E. Traversa, P. Nunziante and G. Chiozzini: *Thermochim. Acta*, 1992, **199**, (1), 25–33.
12. S. Ghosh, R. Majumdar, B. K. Sinhamahapatra, R. N. Nandy, M. Mukherjee and S. Mukhopadhyay: *Ceram. Int.*, 2003, **29**, 671–677.
13. J. Parmentier, M. Richard-Plouet and S. Vilminot: *Mater. Res. Bull.*, 1998, **33**, (11), 1717–1724.
14. P. Kirszensztejn, R. Przekop, A. Szymkowiak, E. Mackowska and J. Gaca: *Micropor. Mesopor. Mater.*, 2006, **89**, 150–157.
15. Z. Haijun, J. Xiaolini, Y. Yongjie, L. Zhanjie, Y. Daoyuan and L. Zhenzhen: *Mater. Res. Bull.*, 2004, **39**, 839–850.
16. S. Mukhopadhyay, S. Sen, T. Maiti, M. Mukherjee, R. N. Nandy and B. K. Sinhamahapatra: *Ceram. Int.,* 2003, **29**, 857–868.
17. B. W. Jong: *Powder Technol.*, 1976,**15**, (1), 135–137.
18. Y. Suyama and A. Kato: *Ceram. Int.*, 1982,**8**, (1), 17–21.
19. T. Suzuki, K. Itatani, M. Aizawa, S. F. Howell and A. Kishioka: *J. Eur. Ceram. Soc.*, 1996, **16**, (11), 1171–1178.
20. G. Ye: 'Reactive processing of ceramic binding systems for refractory castables', PhD thesis, The University of British Columbia, Vancouver, BC, Canada, 2005.
21. T. Yamamura and Y. Kubota: *Taikabutsu Overseas*, 1993, **13**, (2), 39–45.
22. K. Fujii, F. Isao and I. Takita: *Taikabutsu Overseas*, 1992, **12**, (1), 4–9.
23. R. Kockegey-Lorenz, G. Buchel, A. Buhr, J. M. Aroni and R. P. Racher: 'Improved workability of calcia free alumina binder Alphabond for non-cement castables', Proc. 47th Int. Colloq. on 'Refractories', 67–71; 2004, Aachen, Stahl u. Eisen Spezial.
24. Y. Hongo: *Taikabutsu Oversease*, 1989, **9**, 35–38.
25. G. Ye and T. Troczynski: *Ceram. Int.*, 2006, **32**, 257–262.
26. F. A. Cardoso, M. D. M. Innocentini, M. F. S. Miranda, F. A. O. Valenzuela and V. C. Pandolfelli: *J. Eur. Ceram. Soc.*, 2004, **24**, 797–802.
27. M. W. Vance and K. J. Moody: 'Steelplant refractories containing Alphabond hydratable alumina binders', *Alcoa Techn. Bull.*, Oct. 1996, 1–31.
28. T. Yamamura, Y. Hamazaki, T. Kaneshige, T. Toyoda, M. Nishi and H. Kato: *Taikabutsu Overseas*, 1992, **12**, (1), 21–27.
29. M. W. Vance, G. W. Kriechbaum, R. A. Henrichsen, G. Maczura, K. J. Moody and S. Munding: *Bull. Am. Ceram. Soc.*, 1994, **73**, (11), 70–74.
30. Y. C. Ko: *Ceram Int.*, 2002, **28**, 805–810.
31. P. Korgul, D. R. Wilson and W. E. Lee: *J. Eur. Ceram. Soc.*, 1997, (17), 77–84.
32. Y. K. Kalpaklı: Proc.12th Int. Cong. on 'Metalurgy and materials', Istanbul, Turkey, September–October 2005, UCEAT, 1472–1480.
33. M. A. L. Braulio, L. R. M. Bittencourt and V. C. Pandolfelli: *J. Eur. Ceram. Soc.*, 2009, (29), 2727–2735.
34. I. Ganesh, S. Bhattacharjee, B. P. Saha, R. Johnson, K. Rajeshwari, R. Sengupta, M. V. Rao Ramana and Y. R. Mahajan: *Ceram. Int.*, 2002, **28**, 245–253.
35. A. D. Mazzoni, M. A. Sainz, A. Caballero and E. F. Aglietti: *Mater. Chem. Phys.*, 2002, **78**, 30–37.
36. R. Sakar, H. S. Tripathi and A. Ghosh: *Mater. Lett.*, 2004, **58**, 2186–2191.
37. C. Parr, T. A. Bier, M. Vialla and C. Revais: Proc. Cong. Unitecer '99, Berlin, Germany, September 1999, Druckera and Vertag, 19–21.
38. X. Cheng: 'Optimization of magnesia based cement free spinel bonded castables', PhD thesis, University de Montreal, Montréal, Que., Canada, December 1999.
39. R. Sarkar, A. Ghosh and S. Das: *Ceram. Int.,* 2003, **29**, 407–411.
40. G. Brandt and M. Mikus: *Wear*, 1987, **115**, 243–263.
41. M.-K. Cho, G.-G. Hong and S.-K. Lee: *J. Eur. Ceram. Soc.*, 2002, (22), 1783–1790.
42. S. Yılmaz: *Ironmaking Steelmaking*, 2006, **33**, (2), 151–156.